Biliary repair and carcinogenesis are mediated by IL-33–dependent cholangiocyte proliferation

Jun Li,[1] Nataliya Razumilava,[2] Gregory J. Gores,[2] Stephanie Walters,[1] Tatsuki Mizuochi,[1] Reena Mourya,[1] Kazuhiko Bessho,[1] Yui-Hsi Wang,[1] Shannon S. Glaser,[3] Pranavkumar Shivakumar,[1] and Jorge A. Bezerra[1]

[1]Cincinnati Children's Hospital Medical Center and the Department of Pediatrics of the University of Cincinnati College of Medicine, Cincinnati, Ohio, USA. [2]Mayo Clinic College of Medicine, Mayo Clinic, Rochester, Minnesota, USA. [3]Texas A&M Health Sciences Center and Central Texas Veterans Health Care System, Temple, Texas, USA.

Injury to the biliary epithelium triggers inflammation and fibrosis, which can result in severe liver diseases and may progress to malignancy. Development of a type 1 immune response has been linked to biliary injury pathogenesis; however, a subset of patients with biliary atresia, the most common childhood cholangiopathy, exhibit increased levels of Th2-promoting cytokines. The relationship among different inflammatory drivers, epithelial repair, and carcinogenesis remains unclear. Here, we determined that the Th2-activating cytokine IL-33 is elevated in biliary atresia patient serum and in the livers and bile ducts of mice with experimental biliary atresia. Administration of IL-33 to WT mice markedly increased cholangiocyte proliferation and promoted sustained cell growth, resulting in dramatic and rapid enlargement of extrahepatic bile ducts. The IL-33–dependent proliferative response was mediated by an increase in the number of type 2 innate lymphoid cells (ILC2s), which released high levels of IL-13 that in turn promoted cholangiocyte hyperplasia. Induction of the IL-33/ILC2/IL-13 circuit in a murine biliary injury model promoted epithelial repair; however, induction of this circuit in mice with constitutive activation of AKT and YAP in bile ducts induced cholangiocarcinoma with liver metastases. These findings reveal that IL-33 mediates epithelial proliferation and suggest that activation of IL-33/ILC2/IL-13 may improve biliary repair and disruption of the circuit may block progression of carcinogenesis.

Introduction

Disruption of the epithelial lining of bile ducts triggers inflammation and fibrosis, which may manifest clinically as devastating inflammatory diseases in children (e.g., biliary atresia) and adults (e.g., sclerosing cholangitis), or as malignant transformation (e.g., cholangiocarcinoma) at any age. Despite the severe disease phenotypes, the molecular and cellular effectors of bile duct repair and their relationships to mechanisms of carcinogenesis remain largely undefined (1, 2). Studies of pathogenic mechanisms of biliary atresia, the most common end-stage cholangiopathy of childhood, reported that affected livers are populated by lymphocytes at the time of diagnosis (1). In a model of experimental biliary atresia, we found direct evidence that dendritic cells, $CD8^+$ and NK lymphocytes, and their release of IL-15 and IFN-γ are key effectors of biliary epithelial injury (1). While this type 1 immune response is present in most patients with biliary atresia at diagnosis, a previous study reported high levels of Th2 cytokines in a subgroup of patients, including an increased hepatic expression of *IL1RL1*, which encodes ST2, the receptor for IL-33 (3).

IL-33, a member of the IL1 cytokine family, has complex proinflammatory and alarmin functions (4) and has been linked to mechanisms of allergy, autoimmune diseases, and intestinal defense against nematodes, among others (4–7). In the liver, IL-33 appears to be hepatoprotective against Con A and ischemia-reperfusion injury and modulates Treg function in response to HCV infection and chronic fibrosing injuries (8–11). Here, we report an increase in IL-33 in human and murine biliary atresia. Exploring this relationship at the mechanistic level, we found that IL-33 is a potent mitogen to cholangiocytes in vivo, and identified a paracrine system in which type 2 innate lymphoid cells (ILC2s) induce proliferation of the neighboring epithelium by the release of IL-13. The relevance of the IL-33/ILC2/IL-13 circuit in epithelial growth and biliary pathology was demonstrated by the promotion of epithelial repair following tissue injury and by the development of cholangiocarcinoma in mice with genetically primed biliary tract.

Results

IL-33 increases in human and experimental biliary atresia. Based on the previous report of increased expression of *IL1RL1* mRNA encoding the ST2 receptor in the liver at the time of diagnosis of biliary atresia (3), we first quantified the concentration of serum IL-33 in affected subjects. We found an increased serum concentration of this cytokine in 20 patients with biliary atresia (mean ± SD: 218.3 ± 887.0 pg/ml) above undetectable levels of age-matched healthy controls (Figure 1A). In a model of rhesus rotavirus type A–induced (RRV-induced) biliary injury in newborn mice (experimental biliary atresia), the expression of *Il33* mRNA correlated with an increased profile of intrahepatic bile ducts and with the abundance of cholangiocytes in the epithelium of extrahepatic bile ducts (EHBDs) during progression of biliary injury (Figure 1B). In a similar fashion, immunostaining for the St2 receptor showed expression in cholangiocytes along the epithelium of EHBDs in

Conflict of interest: The authors have declared that no conflict of interest exists.
Citation for this article: *J Clin Invest.* 2014;124(7):3241–3251. doi:10.1172/JCI73742.

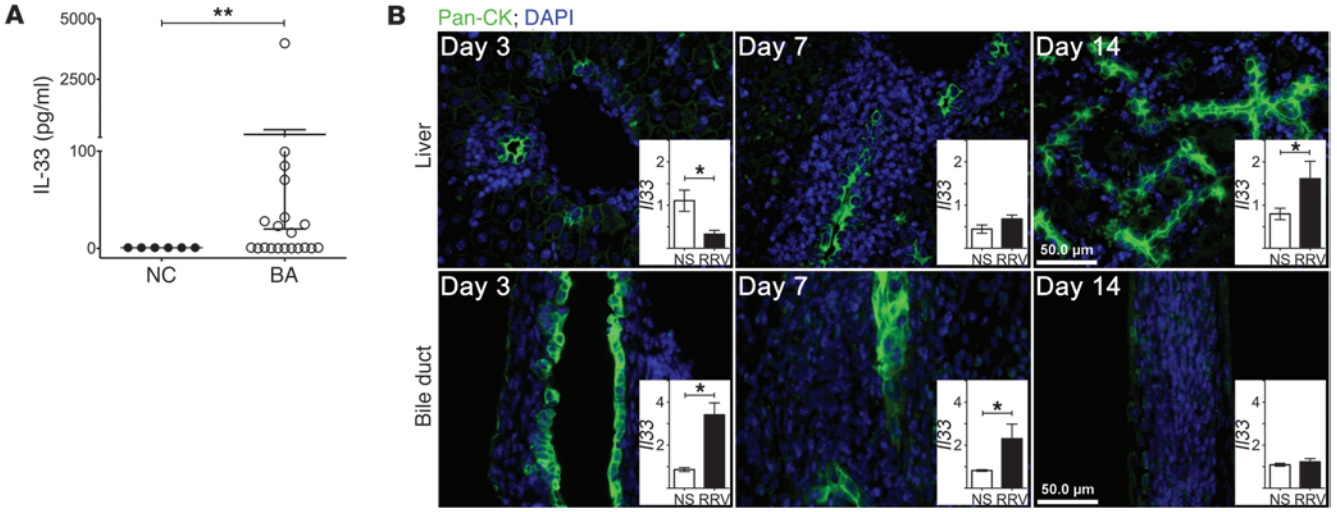

Figure 1

Expression of IL-33 is increased in humans and mice with biliary atresia. (**A**) Serum concentration of IL-33 in infants with biliary atresia (BA) at the time of diagnosis (n = 20, < 4 months of age) and in age-matched normal controls (NC) (n = 6). (**B**) *Il33* mRNA expression (as a ratio to *Hprt*; graphs) and PanCK staining of liver and EHBDs at 3, 7, and 14 days after injection with RRV or normal saline (NS) in the first 24 hours of life. Each time point had n = 4–5 mice for normal saline and RRV groups. Representative immunostaining experiments included tissue sections from 3 mice for each group and time point. Mean ± SD. *P < 0.05; ***P < 0.001. Scale bars: 50 μm.

neonatal mice, with a number of St2$^+$ cholangiocytes decreasing during progression of epithelial injury after rotavirus (Supplemental Figure 1A; supplemental material available online with this article; doi:10.1172/JCI73742DS1). St2 was also expressed in intrahepatic bile ducts (in addition to surrounding hematopoietic cells) in neonatal mice, but the expression decreased after rotavirus challenge and was undetectable in cholangiocytes (Supplemental Figure 1B). In adult mice, St2 was also detected in cholangiocytes of extra- and intrahepatic bile ducts (Supplemental Figure 1C).

To investigate whether IL-33–St2 signaling plays a role in the response of the bile duct to an injury, we injected 0.5 × 10^6 fluorescent focus units (ffu) of rotavirus into newborn mice followed by daily i.p. administration of anti-St2 blocking antibody or IgG isotype (as control) beginning 24 hours later (12). This lower dose of rotavirus induces mild epithelial injury and atresia phenotype in less than 40% of mice. Mice receiving anti-St2 antibody had higher levels of serum alanine aminotransferase and bilirubin after rotavirus challenge than IgG control mice (Figure 2, A and B). Microscopically, mice in the anti-St2 antibody group showed a diffuse loss of the epithelial layer and duct lumen, while controls had a much greater residual epithelial surface area (Figure 2, C–E). The soluble form of St2, which serves as a decoy to neutralize IL-33–induced signaling, increased in the plasma at days 7 and 14 after virus challenge (Supplemental Figure 1D). These data suggested that loss of St2 signaling rendered mice more susceptible to biliary injury and functionally linked the high expression of IL-33–St2 signaling to the abundance of cholangiocytes in the duct epithelium.

IL-33 is a potent epithelial mitogen. To directly determine whether IL-33 induces proliferation of the duct epithelium, we administered 0.1 μg of IL-33 i.p. into newborn BALB/c mice. Measuring proliferation by BrdU incorporation, we found that BrdU$^+$ cholangiocytes of EHBDs increased by approximately 2-fold above the levels of age-matched controls, which had high baseline levels of BrdU incorporation, within 24 hours of injection (Figure 3A). When injected into adult mice, when the baseline cholangiocyte proliferation was less than 1%, 1 μg of IL-33 i.p. increased BrdU uptake by 76-fold in the bile duct epithelium, neighboring peribiliary glands (a site of putative progenitor cells), and cytokeratin-19–negative (CK19$^-$) submucosal cells (Figure 3, A, B, and D). The cholangiocyte proliferation in the epithelium was lower after 4 daily doses, although it remained well above the baseline level (Figure 3B), and was associated with a rise in the plasma concentration of the soluble St2 (Figure 3C). Similar proliferation was achieved with as little as 0.1 μg of IL-33 given to adult mice (Supplemental Figure 2A), and daily administration increased the diameter of EHBDs from 0.3 mm to approximately 3 mm in 1 week, without an obvious effect on the gallbladder (Figure 3, E–G, and Supplemental Figure 2B). In the liver, IL-33 induced cholangiocyte proliferation in hilar bile ducts, but not in small intrahepatic bile ducts in the periphery or in neighboring hepatocytes (Figure 4, A and B). Interestingly, while St2 was expressed in cholangiocytes of intrahepatic bile ducts, the expression was lost after one dose of IL-33 (Figure 4, C and D). In vitro, incubation of IL-33 with human cholangiocyte cell lines induced proliferation if the cells derived from EHBDs (Witt cell line), but not if they derived from intrahepatic bile ducts (H69 cell line) (Figure 4, E–G). These data identified IL-33 as a potent inducer of extrahepatic cholangiocyte proliferation in the absence of preexisting injury. However, the combination of a mild proliferative response in vitro and the inflammatory infiltration in the submucosal compartment suggested that other cellular and molecular signals may be involved in IL-33–induced proliferation.

ILC2s are required for IL-33–induced proliferation of cholangiocytes. The expansion of CK19$^-$ submucosal cells after IL-33 injection provided clues as to their potential role as an amplifier of proliferation. Using flow cytometry, quantification of mononuclear cells showed an increase in basophils and dendritic cells early

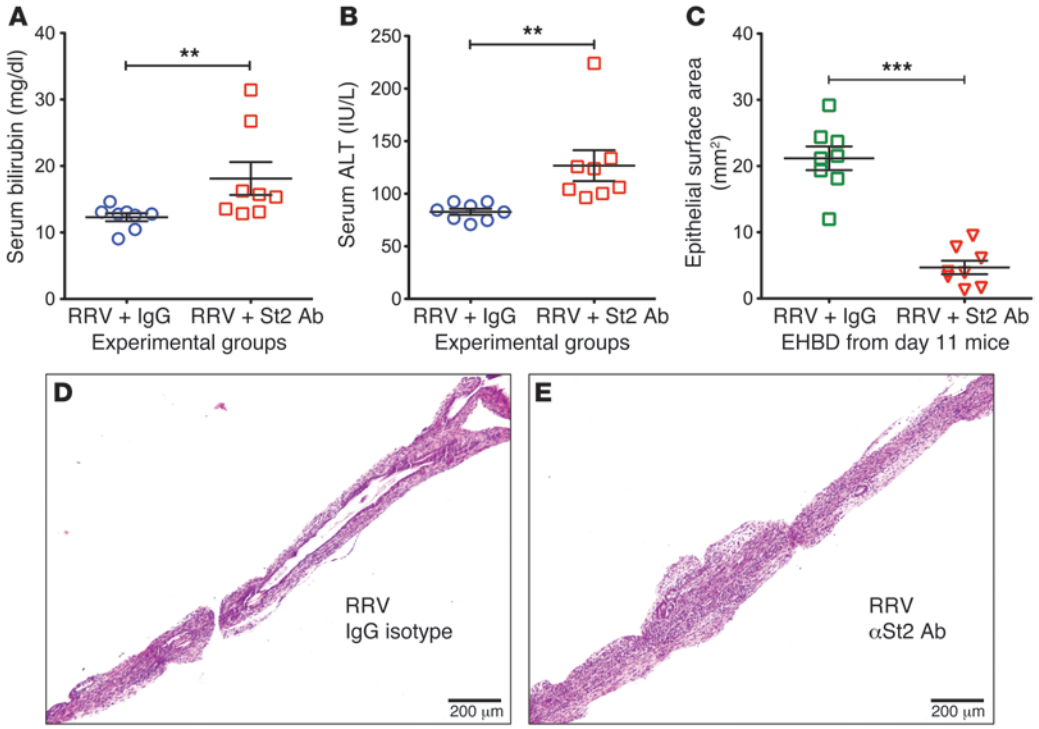

Figure 2

Blocking of St2 by antibodies worsens experimental biliary atresia. Serum levels of bilirubin (**A**) and alanine aminotransferase (ALT) (**B**) increase in mice receiving anti-St2 antibody 7 days after RRV challenge when compared with IgG isotype controls. (**C**) Quantification of the epithelial surface area of EHBDs is significantly smaller in mice receiving anti-St2 than in control mice 11 days after RRV. (**D** and **E**) Representative histological sections show segments of intact epithelium of EHBDs in control mice, but not in anti-St2 mice. $n = 8$ mice for RRV + IgG and $n = 8$ mice for RRV + St2 Ab. Mean ± SD. $^{**}P < 0.01$; $^{***}P < 0.001$. Scale bars: 200 μm.

(1 day) and neutrophils and eosinophils late (4 and 7 days) after IL-33 injection, while a decrease or no change in the number of B, T, and NK lymphocytes was noted after IL-33 injection (Supplemental Figure 3, A and B). Consistent with the ability of IL-33 to promote a Th2 response by activating ILC2s, a type of lineage-negative innate effector leukocyte that expresses the receptor St2 and mediates type-2 immunity (5, 6, 13), liver populations of Lin^-St2^+ cells increased, constituting nearly 50% of the hepatic mononuclear cells by 7 days after IL-33 injection (Figure 5, A–C). Lin^-St2^+ cells (defined by the lack of expression of CD3ε, CD4, CD8α, B220, CD11b, CD11c, CD49b, NK1.1, Gr-1, F4/80, Ter119, and FcεRIα, and expression of St2) expressed surface markers of ILC2s ($CD45^+Sca1^+Icos^+CD127^+CD25^+CD44^+cKit^-Flt3^-$; Figure 5D) and produced progressively increased amounts of IL-13 but not IFN-γ after restimulation with the lymphocyte-activating agents phorbol-12-myristate13-acetate and ionomycin in culture (Figure 5, E and F). These findings formed the basis for the hypothesis that hepatic ILC2 cells and the release of IL-13 mediate the proliferative effects of IL-33.

To directly determine whether ILC2s are required for IL-33–induced proliferation, we injected the cytokine into mice carrying the simultaneous inactivation of the *Rag2* and *Il2rgc* genes ($Rag2^{-/-}gc^{-/-}$ mice); these mice lack ILC2 as well as B, T, and NK cells (Figure 6, A and B, and ref. 14). While IL-33 induced the expected surge of proliferation in epithelial and peribiliary cholangiocytes in C57BL/6 (B6) control mice, bile ducts from $Rag2^{-/-}gc^{-/-}$ mice were completely unresponsive to IL-33 (Figure 6C). In view of the simultaneous loss of other lineage-positive cells in these mice, we adoptively transferred purified ILC2s expressing $CD45.1^+$ from B6/SJL/$CD45.1^+$ mice into $Rag2^{-/-}gc^{-/-}$ mice (expressing $CD45.2^+$) to determine whether ILC2s are responsible for the loss of proliferation (Supplemental Figure 4). Adoptive transfer restored the proliferation of cholangiocytes in the epithelium and peribiliary glands after IL-33 administration to $Rag2^{-/-}gc^{-/-}$ mice (Figure 6, D and E). We applied the same strategy to $Rora^{sg/sg}$ mice, which have a developmental defect in ILC2s, without affecting other immune cell types (15, 16). Cholangiocytes of the EHBDs from $Rora^{sg/sg}$ mice were unresponsive to daily doses of IL-33, while WT controls had the typical surge in proliferation (Supplemental Figure 5, A and B) accompanied by an increase in the number of ILC2s in the liver (Supplemental Figure 5, C and D). Adoptive transfer of bone marrow cells from $Rora^{+/+}$ control mice into $Rag2^{-/-}gc^{-/-}$ mice restored the proliferative response of cholangiocytes to IL-33 administration accompanied by an increase in the number of ILC2s (Supplemental Figure 5, E and F), which did not occur when bone marrow donors were isolated from $Rora^{sg/sg}$ mice (Figure 6F). These data identify ILC2s as key targets of IL-33 and raise the possibility that soluble factor or factors released by these cells may provide proliferative signals to cholangiocytes.

IL-13 mediates IL-33 induced–proliferation of cholangiocytes. Based on the high expression of IL-13 by hepatic ILC2s after IL-33 administration, we quantified IL-13 expression in livers (mRNA) and hepatic mononuclear cells (protein) after IL-33 injection in $Rag2^{-/-}gc^{-/-}$ and $Rora^{sg/sg}$ mice and found it to be increased only after reconstitu-

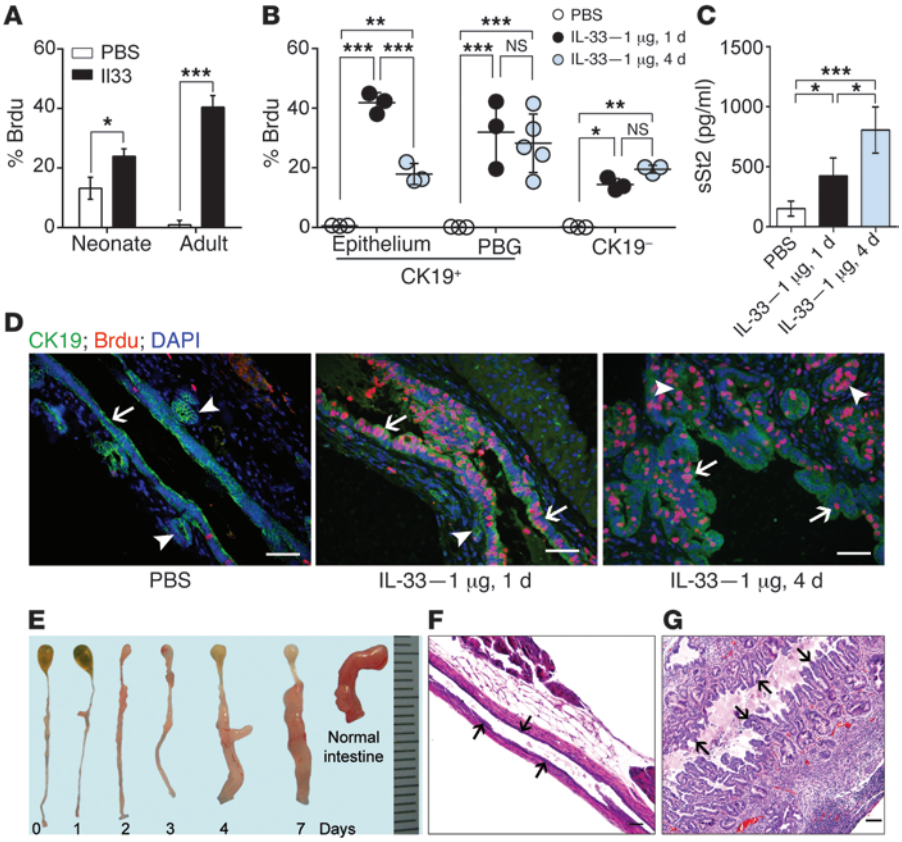

Figure 3

IL-33 induces cholangiocyte proliferation. (**A**) Percentage of CK19⁺ epithelial cells in neonatal and adult EHBDs that stain for BrdU 1 day after PBS or IL-33 (0.1 μg in neonatal and 1 μg for adult mice) i.p. (n = 4 for each group). (**B**) BrdU uptake in CK19⁺ epithelial and CK19⁻ submucosal cells of adult EHBDs after 1 and 4 daily doses of PBS or IL-33. (**C**) Plasma concentration of soluble St2 (sSt2) at the same time points. (**D**) Representative fluorescence images show BrdU uptake by CK19⁺ in epithelium (arrows) and peribiliary glands (PBGs) (arrowheads). (**E**) Representative macroscopic view of EHBDs from adult BALB/c mice after daily doses of IL-33; a segment of normal jejunum is included as a size control. (**F** and **G**) H&E staining of EHBD longitudinal sections after 4 daily doses of PBS or IL-33 shows normal epithelium after PBS (arrows; **F**) and irregular epithelial lining (arrows; **G**) after 1 μg IL-33 due to hyperplasia of duct mucosa, expansion of PBGs, and accumulation of inflammatory cells in the submucosal compartment. Mean ± SD (**A**–**C**) ($n \geq 3$ animals). Experiments shown in **E** were repeated 4 times. $^*P < 0.05$; $^{**}P < 0.01$; $^{***}P < 0.001$. Scale bars: 50 μm.

tion with ILC2s in *Rag2*$^{-/-}$*gc*$^{-/-}$ mice (Supplemental Figure 6A) or in the presence of ILC2s in *Rora*$^{sg/sg}$ mice (Supplemental Figure 6, B and C). Direct i.p. administration of IL-33 to *Il13*$^{-/-}$ mice failed to induce the high BrdU uptake in epithelial and peribiliary cholangiocytes typical of WT mice injected with IL-33, while the proliferative effect on CK19⁻ submucosal cells was similar between *Il13*$^{-/-}$ and WT controls; i.p. administration of IL-13 in a separate group of *Il13*$^{-/-}$ mice restored the increased proliferation of cholangiocytes after injection of 1 μg IL-33 (Figure 7, A and B). Examining whether IL-13 is able to induce cholangiocyte proliferation, we injected increasing amounts of IL-13 i.p. into BALB/c mice. BrdU⁺ cholangiocytes increased with as little as 1 μg, but reached the levels of proliferation induced by IL-33 when the dose reached 20 μg (Figure 7, C and D), a dose previously reported to induce expulsion of *Nippostrongylus brasiliensis* from murine small intestine (17). In vitro, we were unable to detect IL-13 in the conditioned medium from wells containing Witt cells cultured in the presence of IL-33. Additional experiments incubating Witt cells with 10 to 100 ng/ml IL-13 neither induced proliferation nor modified the proliferative response due to IL-33 (Supplemental Figure 7). These data suggest that IL-13 is a secondary signal required for the full proliferative effect of IL-33 in normal cholangiocytes in vivo. However, in experiments with a cholangiocarcinoma cell line, we observed that the mitogenic effect of IL-33 is independent of IL-13.

IL-33 improves the bile duct epithelium in experimental biliary atresia. To investigate the relevance of the proliferative properties of IL-33 to biliary repair and carcinogenesis, we first examined whether the cytokine promotes repair following rotavirus-induced epithelial injury in experimental biliary atresia. The full phenotype was induced by the i.p. administration of 1.5×10^6 plaque-forming units of RRV into BALB/c mice soon after birth (3). Then we injected 0.02 μg IL-33 i.p. daily for 7 days; we used this lower dose because neonatal mice did not tolerate the higher dose, as evidenced by decreased activity in the cage, poor feeding, and a lethargic appearance after repeated administration of 0.1 μg IL-33. On examination of the EHBDs 7 days later, when the bile duct lumen of RRV-infected mice showed inflammatory obstruction and diffuse epithelial loss (which is typical of the

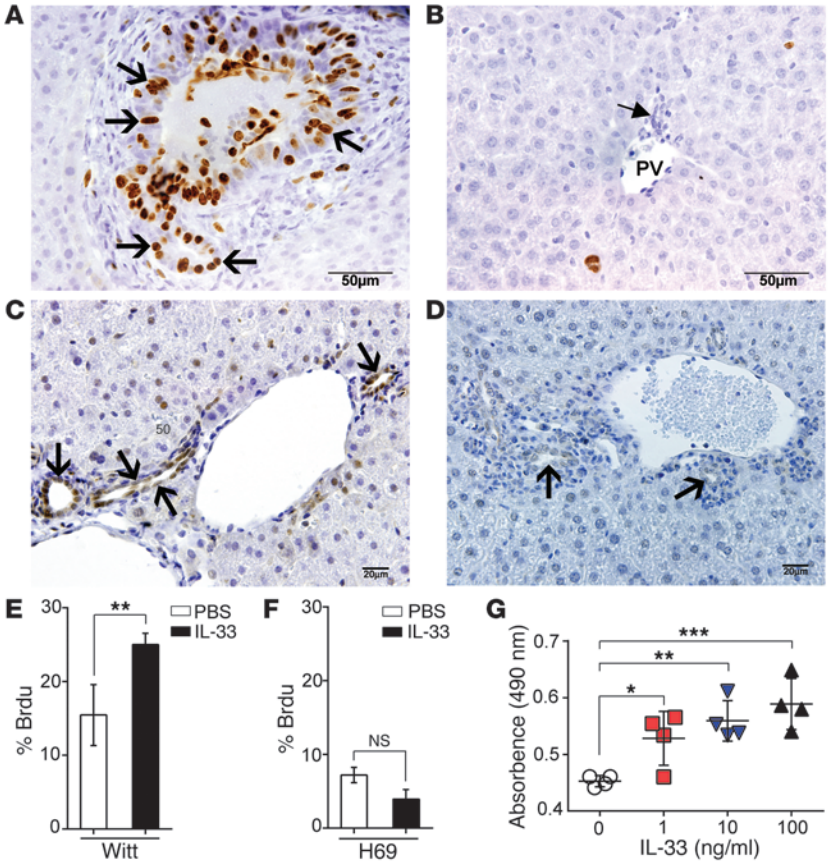

Figure 4
IL-33 induces proliferation of cholangiocytes from hilar bile ducts and a cell line from EHBDs. BrdU staining (brown, arrows) of liver sections after 4 daily doses of IL-33 shows cholangiocyte proliferation in hilar bile duct (**A**), but not in the peripheral small duct (**B**, arrow, bile duct). PV, portal vein. (**C**) Detection of St2 in intrahepatic cholangiocytes by immunohistochemical staining with anti-St2 antibody (brown staining, arrow), which is lost 1 day after 1 dose of 1 μg IL-33 (**D**, arrow). (**E**) BrdU uptake in Witt cells (human extrahepatic cholangiocarcinoma cell line) and (**F**) H69 cells (human intrahepatic duct cell line) after culture with 10 ng/ml IL-33 for 48 hours. (**G**) Witt cell proliferation by the MTS assay after 48 hours of culture with different concentrations of IL-33. Mean ± SD, 4–5 replicates, repeated 3 times. $^{*}P < 0.05$; $^{**}P < 0.01$; $^{***}P < 0.001$. Scale bars: 50 μm (**A** and **B**); 20 μm (**C** and **D**).

disease model; Figure 8, A and C), IL-33 treatment was associated with a patent duct lumen and the epithelium was largely intact, with a much greater surface area than in mice that did not receive IL-33 (Figure 8, B, D, and E).

IL-33 facilitates biliary carcinogenesis. Next, exploring a potential link between IL-33 and biliary carcinogenesis, we injected IL-33 daily into adult BALB/c mice for 10 weeks. Extrahepatic bile ducts increased in size and thickness, largely due to a substantial expansion of peribiliary glands, with remarkable features of glandular metaplasia (Figure 9), raising the possibility that IL-33 requires the activation of other growth-promoting circuits for neoplastic transformation.

Based on the proposed oncogenic roles of Akt and Hippo pathways in the biliary epithelium (18, 19), we investigated whether IL-33 promotes carcinogenesis in mice whose biliary tract is primed to cholangiocarcinoma, the neoplasm originating from cholangiocytes. Genetic priming was induced by the intrabiliary injection of a transposon-transposase complex containing constitutively active Akt (myr-Akt) and Yap (YapS127A) coupled with lobar bile duct ligation to retain the transposon-transposase complex within the bile ducts of B6 mice. Animals received 1 μg of IL-33 or vehicle i.p. for 3 consecutive days and were examined for tumor burden and tumor characteristics 8 weeks later. In the group of animals that received both the transposons and IL-33, 10 of 17 (or 58.8%) mice developed advanced tumors with intrahepatic metastases (Figure 10, A and B) as compared with none of the animals in the group injected with transposons without IL-33 ($n = 4$, $P < 0.05$). The livers containing cancer had an average of 38 ± 9.4 macroscopic nodules, with the nodule size averaging 1.3 ± 0.07 mm. Microscopically, tumor nodules were easily identifiable by H&E staining in a background of normal liver (Figure 10C). Intrahepatic tumors exhibited neoplastic glands that strongly expressed pAkt and Yap (the activated forms of the oncogenes), and the 2 markers of biliary differentiation pancytokeratin (PanCK) and Sox9, without expression of HepPar1, a marker of hepatocellular cells (Figure 10C). Thus, exogenous administration of IL-33 to genetically susceptible mice potentiates oncogene-associated biliary tract carcinogenesis.

Discussion

The findings of increased IL-33 in children with biliary atresia and its correlation with bile duct hyperplasia in a murine model of the disease suggested a potential link between the cytokine and cholangiocyte biology. Exploring this link, we produced direct evidence that IL-33 triggers cholangiocyte proliferation and epithelial hyperplasia in mice. This proliferative response depends largely on the presence of ILC2s and on the expression of IL-13, a cytokine with Th2 properties, as supported by a substantial reduction in proliferation when mice are engineered to lack ILC2s or IL-13. In normal mice, the epithelial hyperplasia induced by IL-33 increased the diameter of EHBDs without preexisting injury. In experimental biliary atresia, antibody blocking of IL-33r rendered newborn mice more susceptible to bile duct injury induced by rotavirus, while IL-33 administration suppressed the phenotype and restored the duct epithelium. Further, in a model of experimental carcinogenesis, IL-33 injection into mice with active Akt and Hippo pathways

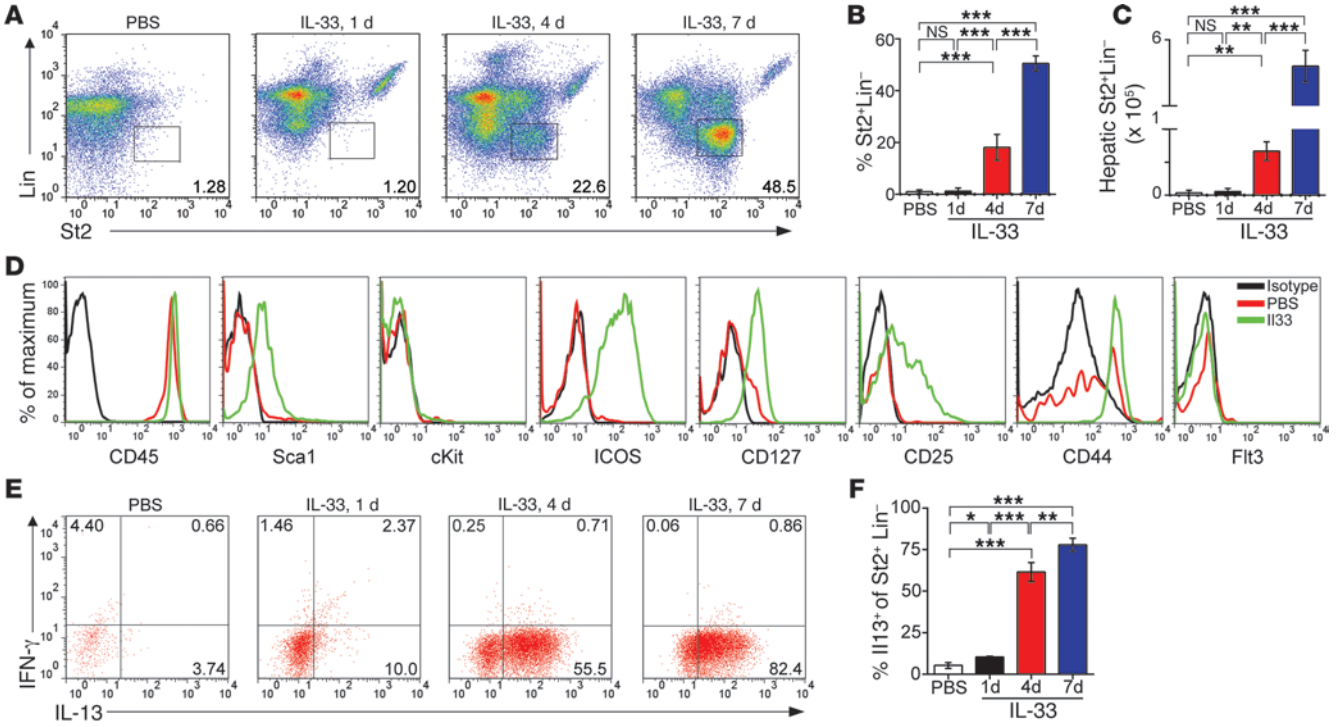

Figure 5

Hepatic ILC2s increase after IL-33 treatment. Representative dot plots (**A**) and quantification from 3 independent experiments (**B** and **C**) of flow cytometric assays show that hepatic ILC2s increase after 4 and 7 days of IL-33 injection. (**D**) By gating on Lin$^-$ST2$^+$ cells, plots show that IL-33 upregulates the expression of Sca1, ICOS, CD127, CD25, and CD44, but not that of CD45, cKit, or Flt3 (Flt3$^-$). (**E** and **F**) Intracellular staining shows ILC2 cells harvested from livers at the specified time points after daily injections of IL-33 produce high levels of IL-13 and minimal amounts of IFN-γ after restimulation with phorbol 12-myristate 13-acetate and ionomycin in vitro for 4 hours. Data in **C** are absolute cell count at specified time points, **E** contains representative dot plots, and **F** shows percent of ILC2s expressing IL-13 from 3 independent experiments. Mean ± SD, 4–5 replicates. $^*P < 0.05$; $^{**}P < 0.01$; $^{***}P < 0.001$.

in the biliary system facilitated the development of cholangiocarcinoma. Collectively, the findings identify IL-33 as an activator of a paracrine circuit that regulates cholangiocyte proliferation, with preliminary proof-of-principle experiments that point to relevance to tissue growth, inflammation, biliary repair, and carcinogenesis.

The biological effects of the IL-33/ILC2/IL-13/cholangiocyte circuit are unexpectedly restricted to EHBDs and hilar bile duct branches and broadly apply to cholangiocytes in the epithelium and peribiliary glands. We don't yet know the biological basis for a proliferative response that is restricted to cholangiocytes of EHBDs. This regional responsiveness suggests the existence of unique biological properties of EHBDs that differ from intrahepatic bile ducts. The concept is supported by previous reports identifying the requirements of *Sox17* in the establishment of distinct anatomical boundaries among the liver, bile ducts, and pancreas (20). Further, the genetic inactivation of the genes *Lgr4* or *Hes1* causes abnormal development of different segments of the EHBD system without affecting intrahepatic bile ducts (reviewed in ref. 1). Our findings differ from the indirect protection of the liver described for IL-33 following ischemia/reperfusion injury or viral insult, which has been linked to a differential effect on regulatory T lymphocytes, dendritic cells, and macrophages (9, 10) or to profibrogenic properties in the liver (11). These differences notwithstanding, the studies point to IL-33 as a soluble factor with both protective and reparative properties in the liver and biliary system.

From an immune perspective, the role of ILC2s as cellular sensors and effectors for IL-33 is in keeping with their functional relationship with other systems (respiratory and gastrointestinal), where they fulfill different biological end points (bronchial reactiveness and helminth expulsion, respectively) (5, 6, 12, 13, 21–23). ILC2s are involved in immunity and produce IL-5 and IL-13 upon IL-33 stimulation. They are increasingly recognized as playing important role(s) in tissue injury and intestinal defense (5, 6, 14, 22–25). In the liver, the profibrogenic properties reported recently (11) differ from our findings in that IL-33 has a reparative dimension by promoting proliferation of cholangiocytes and repair of the duct epithelium. These differences may be related, at least in part, to distinct biological signals activated by IL-33 in the liver versus EHBDs and to the diverse types of injury models. Although we have not formally investigated the role of IL-33 in the production of the extracellular matrix in EHBDs, it is possible that IL-33 may aid tissue repair by promoting the expression of matrix components as well as epithelial proliferation. We recognize, however, that additional studies are needed to investigate these seemingly diverse and complementary processes.

We reported previously that the overactivation of Th2 signals, and specifically those of IL-13, allows for the development of epithelial injury and biliary inflammation following rotavirus infection of newborn mice (3). Despite the functional relatedness of IL-13 with IL-33, administration of IL-33 is protective to the bile duct epithelium. One of the potential reasons for this discrepancy is that the

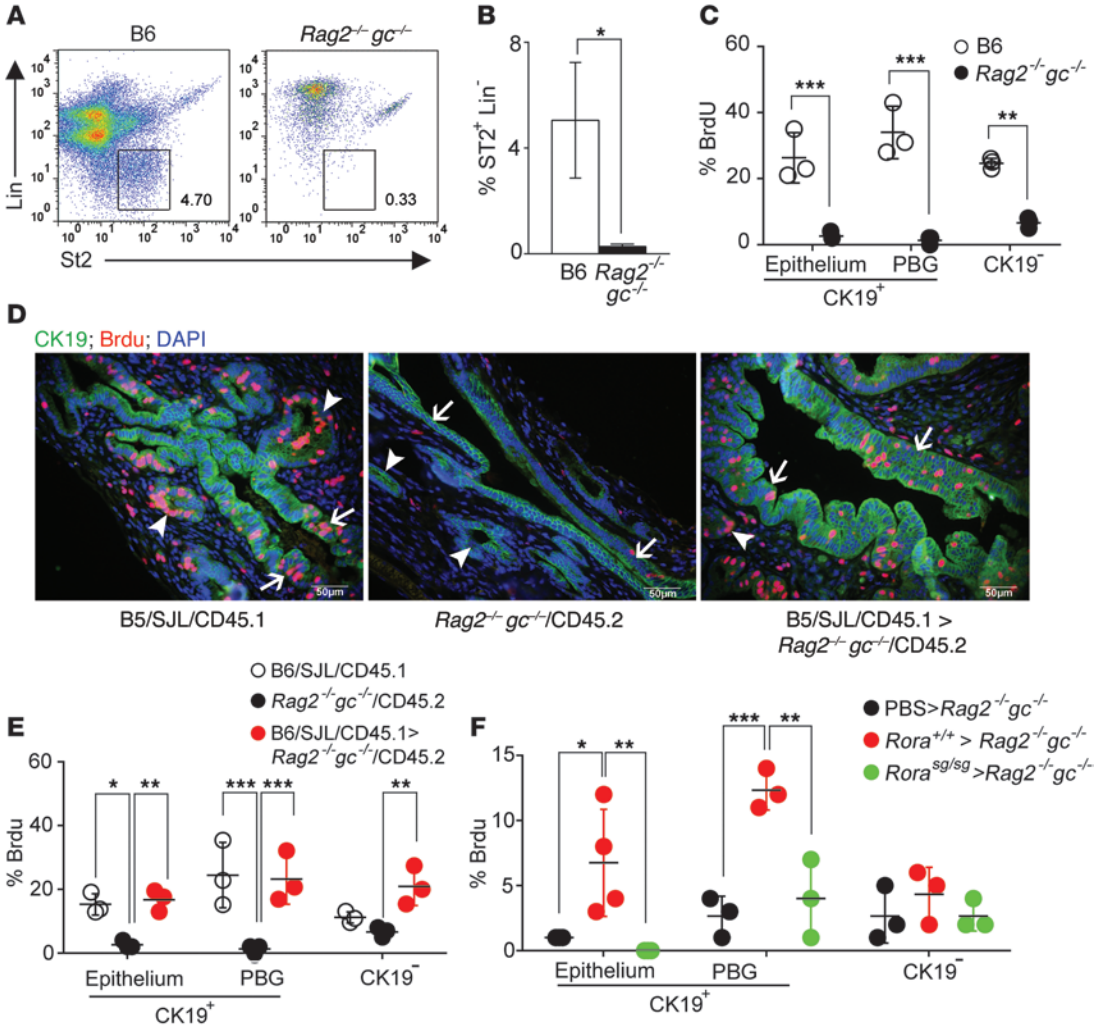

Figure 6

ILC2s mediate IL-33–induced cholangiocyte proliferation. (**A**) Representative dot plots show that *Rag2*$^{-/-}$*gc*$^{-/-}$ mice lack Lin$^-$ST2$^+$ population after 4 days of IL-33 injections (B6 strain used as control). (**B**) Quantification of Lin$^-$ST2$^+$ cells from total hepatic mononuclear cells from 3 independent experiments. (**C**) Quantification of BrdU uptake by CK19$^+$ and CK19$^-$ cells in EHBDs by immunofluorescence staining 1 day after administration of IL-33 into *Rag2*$^{-/-}$*gc*$^{-/-}$ mice compared with B6 controls. (**D**) BrdU staining showing the recovery of proliferation in EHBDs of *Rag2*$^{-/-}$*gc*$^{-/-}$ mice following adoptive transfer of B6/SJL/CD45.1$^+$ Lin$^-$ST2$^+$ cells after IL-33, with (**E**) quantification of BrdU uptake. (**F**) BrdU uptake in EHBDs of *Rag2*$^{-/-}$*gc*$^{-/-}$ mice after i.p. administration of PBS or 5 × 10^6 bone marrow cells from *Rora*$^{+/+}$ or *Rora*$^{sg/sg}$ mice into *Rag2*$^{-/-}$*gc*$^{-/-}$ mice, followed by IL-33 treatment i.p. for 6 weeks. Mean ± SD. **P* < 0.05; ***P* < 0.01; ****P* < 0.001. Scale bars: 50 μm.

previous experimental approach used BALB/c mice with a congenital inability to mount a Th1 response due to the inactivation of the *Stat1* gene. In such a setting, rotavirus triggered the antivirus response from a default Th1 to an IL-13–rich response and a tissue infiltration of type 2 inflammatory cells that obstruct the bile ducts (3). In contrast, the biliary injury in our experiments, typically accompanied by a type 1 response (1), was substantially decreased by the administration of IL-33, suggesting that the IL-33–induced activation of innate lymphoid cells may act to protect or repair the duct epithelium. In humans, the combination of the increased expression of IL-13, IL-33, and the IL-33 receptor when the disease is fully established suggests a potential sequence of events in which the biliary environment transitions from the initial proinflammatory response that injures the epithelium to a reparative type 2 response in an attempt to reconstitute the biliary epithelium.

The powerful proliferative stimulus linking IL-33, ILC2s and IL-13 to neighboring cholangiocytes in vivo is far superior to the proliferation provided by hepatocyte growth factor, epidermal growth factor-signaling, and other mitogens (26). The mechanisms used by IL-13 to mediate the effect of IL-33 may involve the IL-4Rα (an important component of the heterodimeric IL-13 receptor) and the downstream target of Stat6 (11). Future studies to formally dissect this molecular mechanism will be important in view of our findings that daily administration of IL-33 produces metaplastic changes. Additional studies will also be needed to investigate the molecular synergy that facilitated malignant transformation, with the development of cholangiocarcinoma and intrahepatic metastasis when it was administered, even on a short-term basis, to mice engineered to have a simultaneous activation of Akt and Hippo pathways. While we cannot rule out

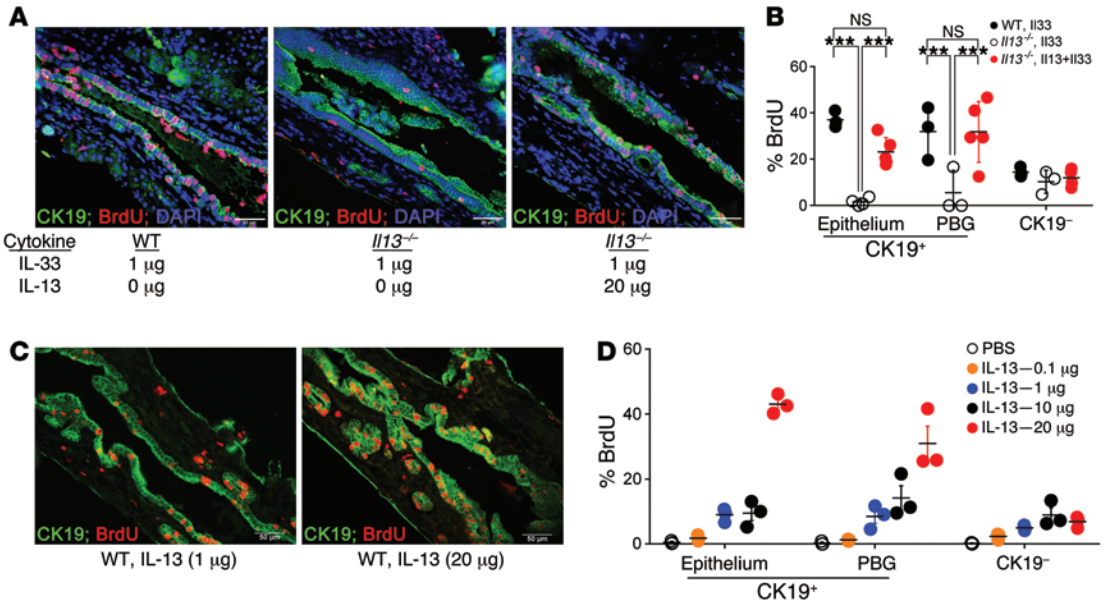

Figure 7

IL-13 as a molecular effector of IL-33–induced proliferation. Fluorescence images (**A**) and percentage of BrdU uptake from 3 to 5 animals (**B**) in representative sections of EHBDs 1 day after injection of IL-33 and/or IL-13 into WT or *Il13*$^{-/-}$ mice. (**C** and **D**) Percentage of BrdU cells after different doses of IL-13 in representative EHBDs (**C**) or quantification from 3 animals (**D**) 1 day after injection of 0.1, 1, 10, and 20 μg of IL-13 into WT mice. Mean ± SD. ***$P < 0.001$. Scale bars: 50 μm.

the possibility that IL-33 can independently induce malignant transformation of the biliary epithelium if administered daily for more than 10 weeks, we found evidence that IL-33 induced proliferation of a human cholangiocarcinoma cell line (Witt cells) independently of IL-13. It is possible that the transformed phenotype of Witt cells renders them susceptible to IL-33, which does not apply to the bile duct epithelium of normal mice. Collectively, our data clearly point to a potential biological synergy among IL-33, Akt, and Hippo, which appear to be complementary pathways in pathogenesis of cholangiocarcinoma.

In summary, experiments to investigate the biological relevance of increased IL-33 in children with biliary atresia identified the protein as a potent inducer of bile duct epithelial hyperplasia. The hyperplastic response resides largely in cholangiocytes and is regulated by neighboring ILC2s and the release of IL-13. Combined, the IL-33/ILC2/IL-13/cholangiocyte circuit may represent an important physiologic driver of tissue repair and, when in a favorable pathologic setting, a facilitator of biliary carcinogenesis. Thus, IL-33 or elements of the paracrine circuit may be manipulated to augment tissue repair or may constitute potential new therapeutic targets against cholangiocarcinoma.

Methods

Mouse lines and experimental challenges. Experimental mice were age and sex matched and of BALB/c background unless otherwise specified. BALB/c and B6 mice were purchased from Charles River Laboratories. B6/SJL (CD45.1$^+$ congenics) and B6 *Rag2*$^{-/-}$*Il2rgc*$^{-/-}$ mice were from Taconic Laboratories, while B6 *Rora*$^{+/sg}$ mice were purchased from the Jackson Laboratory. We generated *Rora*$^{sg/sg}$ mice in our laboratory by successive matings of heterozygous mice and identified targeted genes by PCR using tail DNA according to protocols from the providers of the mouse strains. *Il13*$^{-/-}$ BALB/c mice were generated in the laboratory of Andrew N.J. McKenzie (MRC Laboratory of Molecular Biology, Cambridge, United Kingdom) and a gift from Marc E. Rothenberg (Cincinnati Children's Hospital Medical Center). For in vivo experiments, IL-13 or IL-33 was injected to mice i.p. daily with specified dose and timing.

Mouse model of biliary atresia. Experimental biliary atresia was induced in neonatal BALB/c mice by inoculation of 0.5 or 1.5 × 10^6 ffu of RRV i.p. in the first 24 hours as described previously (3). Mice injected with 0.9% NaCl (saline) solution served as controls. For IL-33 studies, 0.02 μg of murine IL-33 was injected daily until day 7 of life; control mice received an equivalent amount of protein (1% BSA). For IL-33r (St2) blocking, neonatal mice were challenged with 0.5 × 10^6 ffu of RRV followed by injections of 20 μg of anti-mouse St2/IL-1R4 antibodies (R&D Systems) every other day until day 10 of life; control mice received rat anti-mouse IgG2b antibodies. Livers, EHBDs, and gallbladders were microdissected en bloc at days 7 (IL-33) and 11 (IL-33r) after RRV challenge. The epithelial surface area of cholangiocytes along the entire length of the common bile duct was morphometrically determined using H&E-stained consecutive sections and expressed as mm^2. Data for surface area calculations were gathered at ×100 to ×200 magnification and used the Count-and-Measure feature of the Cellsens 1.9 (Dimension Package) digital imaging software (Olympus America Inc.).

Cell lines and in vitro proliferation study. We used the cholangiocarcinoma cell line Witt (Sk-ChA-1), derived from a patient with extrahepatic cholangiocarcinoma, and a human immortalized nonmalignant cholangiocyte cell line H69 (from D.M. Jefferson, Tufts University School of Medicine, Boston, Massachusetts, USA). They were cultured as described (27, 28). For MTS (3-[4,5-dimethylthiazol-2-yl]-5-[3-carboxymethoxyphenyl]-2-[4-sulfophenyl]-2H-tetrazolium, inner salt) cell proliferation assays, cell lines were seeded into 96-well plates (10,000 cells per well) in a final volume of 100 μl of growth medium for 48 hours and then were serum starved for 48 hours before stimulation with IL-33 and/or IL-13. After incubation for 48 hours, cell proliferation was assessed using a colorimetric cell proliferation assay (CellTiter 96Aqueous; Promega), and absorbance was measured at 490

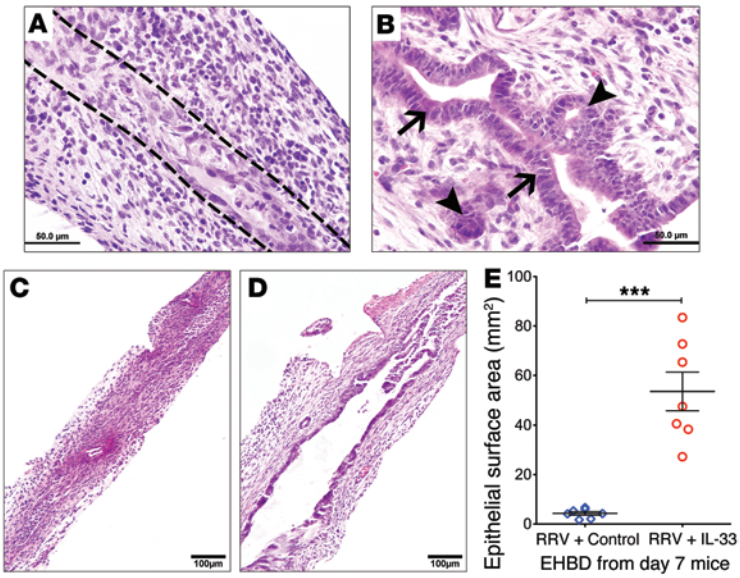

Figure 8
IL-33 promotes epithelial repair in experimental biliary atresia. The epithelial injury and lumen obstruction of EHBD 7 days after rotavirus (RRV) infection (**A**; dashed lines depicts obstructed duct lumen) are prevented in mice that also receive daily doses of 0.02 μg IL-33 (**B**; arrows show epithelium; arrowheads show peribiliary glands). Quantification of the surface area of the mucosal lining of EHBDs from RRV-infected mice followed by daily doses of PBS (**C**, as control) or IL-33 (**D**) for 7 days shows a greater abundance of epithelium in the IL-33 group (**E**). Mean ± SD. ***$P < 0.001$. Scale bars: 50 μm (**A** and **B**); 100 μm (**C** and **D**).

nm by a microplate reader (Synergy H1 Hybrid Reader; BioTek). For BrdU incorporation assays, cells were treated as above, and BrdU was added to the cells 2 hours prior to BrdU staining. Cells were then collected from 3 replicates, and the incorporated BrdU was measured according to instructions included in the APC-conjugated BrdU Flow Kit (BD Bioscience).

Antibodies and reagents. Recombinant mouse and human IL-13 were from PeproTech; recombinant mouse and human IL-33 were from BioLegend. The following primary antibodies were used for flow cytometry: FITC-conjugated anti-CD4 (RM4-5) and anti-CD3 (17A2); PE-conjugated anti-Siglec-F (E50-2440), and CD45.1 (A20); PerCP-conjugated anti-CD4, CD8a (53-6.7), and B220 (RA3-6B2); APC-conjugated anti-Ckit (2B8), CD25 (PC61), CD44 (1M7), CD45.2 (clone 104), Siglec-F (E50-2440), and IFN-γ (XMG1.2); and purified anti-FcRII/III (CD32/CD16; 2.4G2), from BD Biosciences. FITC-conjugated anti-CD11b (M1/70); PE-conjugated anti-CD19 (eBio1D3), CD127 (A7R34), FcεRIα (MAR-1), F4/80 (BM8), Sca-1 (D7), and IL-13 (eBio13A); PerCP Cy5.5-conjugated anti-CD11b (M1/70), Gr-1 (RB6-8C5), and TER-119 (TER-119); APC-conjugated anti-CD45 (30-F11), CD49b (DX5), Flt3 (A2F10), and Sca-1 (D7) were from eBiosciences. PE-conjugated anti-CD45 (30-F11); PerCP-conjugated anti-CD3ε (145-2C11); PerCP Cy5.5 conjugated anti-CD11c (N418), CD49b (DX5), F4/80 (BM8), FcεRIα (MAR-1), and NK1.1 (PK136); APC-conjugated anti-ICOS (398.4A) and Alexa Fluor 647–conjugated anti-CCR3 (TG14/CCR3) were purchased from BioLegend. FITC-conjugated anti-T1/ST2 (DJ8) was from MD Bioproducts. Lineage cocktail included PerCP-conjugated anti-CD3ε, anti-CD4, anti-CD8α, anti-B220 and PerCP Cy5.5 conjugated anti-CD11b, anti-CD11c, anti-CD49b, or NK1.1, Gr-1, F4/80, Ter119 and FcεRIα. BrdU solution was purchased from BD Biosciences. For immunohistochemistry staining, biotin anti-BrdU antibody was from Abcam. The Rabbit IgG Vectastain ABC Kit was used according to the manufacturer's recommendations for blocking, antibody incubations, and signal amplification (Vector Laboratories). Purified anti-CK19 antibody was from Santa Cruz Biotechnology Inc. Anti-PanCK antibody was purchased from Dako. DyLight 488–conjugated donkey anti-goat and DyLight 594–conjugated streptavidin antibodies were from Jackson Immunoresearch. ProLong Gold antifade reagent with DAPI for nuclear staining was from Invitrogen.

Cell isolation. To obtain hepatic mononuclear cells, liver cell dissociation was done using gentleMACS Dissociator (Miltenyi Biotec) according to then manufacturer's manual. Single-cell suspensions were then obtained by passing the cells through a 40-μm strainer and centrifugation in 33% Percoll at 836 *g*, 20°C for 20 minutes; they were then washed twice in complete DMEM (Biowhittaker), subjected to red cell lysis buffer, and used in flow cytometry. Bone marrow cells were collected by flushing the femurs and tibias from mice with complete DMEM. The single-cell suspension was washed twice with complete DMEM, immersed in red cell lysis buffer, and then washed and stained for flow cytometric analysis or ILC2 isolation for cell culture or adoptive transfer experiments.

Flow cytometry and cell sorting. According to established protocols (29), cells were resuspended in PBS containing 1% BSA and then incubated at 4°C for 30 minutes with combinations of fluorochrome-conjugated anti-

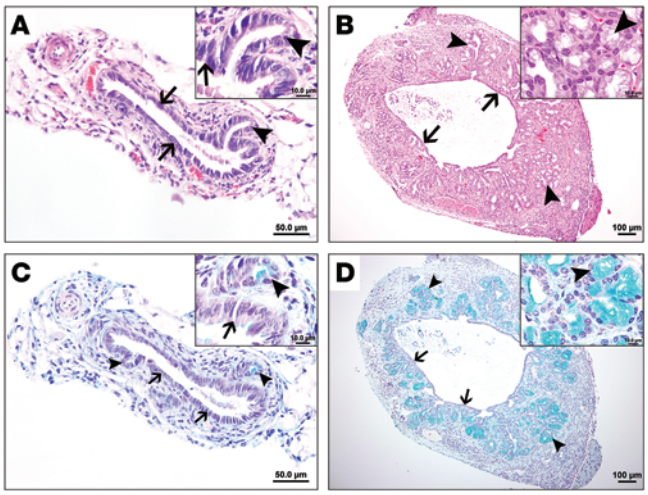

Figure 9
Long-term administration of IL-33 promotes epithelial metaplasia. Cross sections of a representative adult mouse EHBD before (**A**) and after (**B**) 10 weeks of daily injections of IL-33 show glandular metaplasia. (**C** and **D**) Cross sections stained with Alcian blue show intense staining in abundant peribiliary glands. Arrows show bile duct epithelium, and arrowheads point to peribiiary glands. Scale bars: 50 μm (**A** and **C**); 100 μm (**B** and **D**).

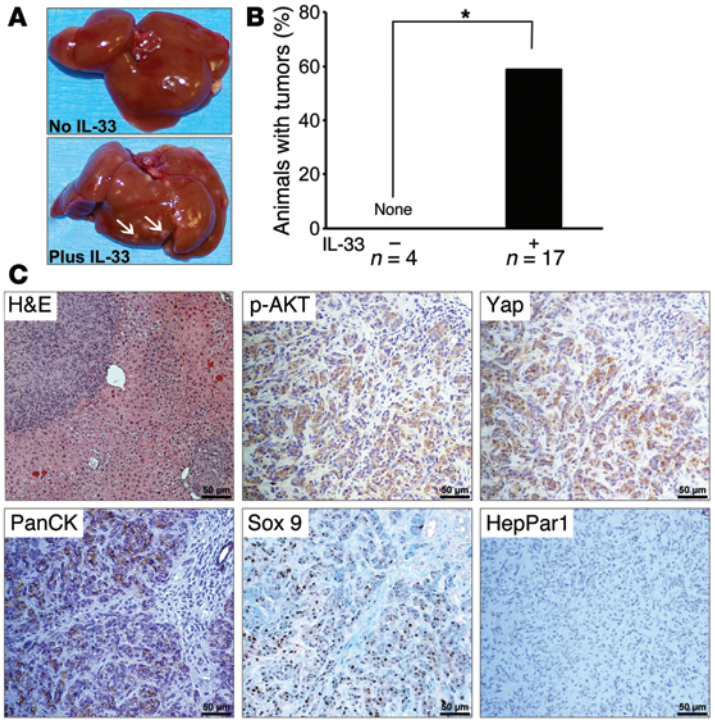

Figure 10
IL-33 facilitates biliary carcinogenesis. (**A**) liver appearance of mice after intrahepatic injection of myr-Akt and YapS127A Sleeping Beauty transposon-transposase complexes coupled with lobar bile duct ligation, and without (upper photo) or with (lower photo) daily injections of IL-33 (1 μg i.p. for 3 days). The lower photo shows liver nodules (arrows) representing neoplasms in mice with constitutively active Akt and Yap and injection of IL-33. (**B**) Percentage of animals with liver tumors (*$P < 0.05$). (**C**) Intrahepatic neoplastic nodules stained by H&E; expression of p-AKT; Yap; PanCK, and Sox 9 (nuclear staining), markers of biliary differentiation; and negative staining for HepPar1, a hepatocyte marker. Scale bars: 50 μm.

bodies. For intracellular staining of cytokines, cells were stimulated with 5 ng/ml PMA and 750 ng/ml ionomycin (Sigma-Aldrich) in the presence of 1 μl/ml GolgiPlug (BD Biosciences) for 4 to 5 hours (29). Cells were then harvested, washed, and stained with antibodies to surface markers, washed, and blocked with purified anti-FcRII/III (CD32/CD16; 2.4G2, BD Biosciences), followed by incubation with the BD Cytofix/Cytoperm kit (BD Biosciences — Pharmingen) for 30 minutes and anti-cytokine antibodies at 4°C. Cells were analyzed on a FACSCalibur or FACSCanto (BD Biosciences) or were purified with an Ariel cell sorter (BD FACSAria II) according to the manufacturers' standard operating procedures. Data were analyzed with FlowJo software, version 7.6.5.

Adoptive transfer experiments. Lin^-ST2^+ ILC2s were sorted from pooled total hepatic mononuclear cells isolated from 3 to 4 mice at 6 to 8 weeks of age after 4 days of IL-33 treatment. Purified 1×10^5 ILC2s were resuspended in 100 μl PBS and injected into the recipient mice i.p. For bone marrow cell transfers, 5×10^6 cells in 100 μl PBS were given i.p. The second day, 1.0 μg IL-33 was given to the transplant recipient mice i.p. for the specified duration.

Oncogenic transposon injection into the biliary tree. B6 mice were anesthetized by pentobarbital injections of 40 to 85 mg/kg i.p. Under deep anesthesia, the abdominal cavity was opened by a midline approach, and the liver was gently retracted and allowed to rest on the diaphragm temporarily. The common bile duct located below the liver was clamped with a small-animal surgical clip to prevent the injected material from flowing into the duodenum. The bile duct draining the left lateral liver lobe was identified, and a ligature (6.0 silk) was placed loosely around the duct. Another ligature was placed around the base of the gall bladder where it meets the cystic duct. 100 μl of the plasmid solution in in vivo jetPEI (Polyplus) prepared according to the manufacturer's instructions was injected into the gall bladder with enough pressure to allow the solution to distend the liver biliary system. A sterile cotton-tipped applicator was held over the injection site for about a minute to prevent leakage. The ligature around the left lateral liver lobe duct was then tied off so as not to allow the plasmid solution to flow from this bile duct to the common bile duct. Following plasmid injection and the left lateral bile duct ligation, the common bile duct was unclamped. The ligature around the base of the gall bladder was then tied off and a cholecystectomy performed. Internal organs were returned to their original position. The abdominal wall and skin were closed in a separate layers pattern with absorbable chromic 3-0 gut suture material. Then each animal was injected with 1 μg of IL-33 (R&D Systems) i.p. starting on day 1 for 3 days. Animals were euthanized 8 weeks later and examined for the presence of tumor and metastases.

Transposon-transposase complex. myr-AKT with N-terminal HA tag plasmid, YapS127A-containing plasmid, and hyperactive Sleeping Beauty transposase-containing plasmid (pCMV-SB) were a gift of Xin Chen (UCSF, La Jolla, California, USA). Both AKT and Yap are expressed from the EF1α promoter. Hyperactive Sleeping Beauty transposase is expressed from the CMV promoter. AKT (11 μg) plus Yap (11 μg) plasmids were combined with Sleeping Beauty transposase (3 μg) plasmid, diluted in 100 μl 0.9% NaCl, sterile filtered, and injected into the biliary system as described above.

Histology and immunostaining. Sections of parafin-embedded livers and bile ducts were stained with H&E or Alcian blue. For immunofluorescence studies, sections were stained with antibodies for rabbit PanCK or goat CK19 (1:100), followed by DyLight 488–conjugated donkey anti-goat antibodies (1:1000), then incubated in biotinylated anti-BrdU antibody (1:200) overnight at 4°C, and finally in DyLight 594–conjugated streptavidin (1:1000). Slides were coverslipped with ProLong Gold antifade reagent with DAPI and examined by fluorescence microscopy. Color was developed using the DAB peroxidase substrate kit (Vector Laboratories) and hematoxylin counterstaining. Citric acid buffer (pH = 6) was used for BrdU. $CK19^+$ in epithelium or PBGs and $CK19^-$ cells from well-oriented EHBDs were counted at ×40 magnification, followed by counts of BrdU-positive cells. The percentage of BrdU-positive $CK19^+$ epithelial cells, $CK19^+$ PBGs, or $CK19^-$ cells was determined for each animal (at least 500 cells per genotype were counted for each animal).

Additional immunostaining was performed using antibodies to the following proteins: p-Akt and Yap (rabbit species, at 1:150 and 1:25 dilutions, respectively; Cell Signaling), PanCK (rabbit species, 1:40; Dako), Sox-9 (rabbit species, 1:1000; Millipore), HepPar1 (mouse species, 1:40; Thermo Scientific), and St2 (rabbit species, 1:200; AbCam). All antigen -retrieval procedures were performed with the citrate buffer. Blocking was performed with 5% BSA blocking buffer (or using the Mouse-on-Mouse Kit from Vector Laboratories for anti-HepPar1 antibody). Primary antibodies were diluted in 1% BSA where applicable. Peroxidase rabbit IgG kit was used for staining development to detect St2/IL-33r, and Dako EnVision kit was used to detect all other secondary antibodies. Hematoxylin was used for counterstaining in assays for p-AKT, Yap, PanCK, HepPar1, and St2; blue cytoplasm counterstaining (Accurate Chemical and Scientific Corporation) was used for the Sox9 detection assay.

Real time PCR analysis. RNA isolation, cDNA synthesis, and quantitative PCR amplification using the Brilliant III SYBR Green QPCR Master Mix gene expression assay kit and the Mx3005P system (Stratagene, Agilent Technologies) were performed as described previously (3). Primers for *Hprt* and *Il13* were published in our previous study (3); other primers used were as follows: mouse *Il33* sense (5′-TCCTTGCTTGGCAGTATCCA-3′) and mouse *Il33* antisense (5′-TGCTCAATGTGTCAACAGACG-3′) (30). mRNA expression of target genes was normalized to the endogenous reference *Hprt* gene.

Concentration of human IL-33 and mouse St2 in serum or plasma. The concentration of cytokines was measured in serum from 20 children with biliary atresia at the time of diagnosis (<4 months of age) and from 6 age-matched healthy infants using the Luminex technology platform (Millipore). Mouse plasma was collected in BD Microtainer tubes with EDTA (BD Bioscience) followed by centrifugation at 2,655 *g* for 10 minutes. Supernatants were saved at –80°C until the time of analysis. Plasma sSt2 was detected following the manufacturer's protocol using the Mouse St2 (IL-33r) ELISA Ready-SET-Go! Kit.

Statistics. All in vitro experiments were performed at least in triplicate. The numbers of mice or tissues used in each experiment are presented in the text or figure legends. Values are expressed as mean ± SD, and statistical significance was determined by 2-tailed Student's *t* test, Wilcoxon signed rank test, or by 1-way or 2-way ANOVA for comparison between 3 or more groups, with a significance set at $P < 0.05$.

Study approval. The Institutional Animal Care and Use Committee of Cincinnati Children's Hospital Medical Center approved the experimental protocols for the mouse experiments. Subjects with biliary atresia or age-matched healthy controls were enrolled into a study protocol after obtaining signed consent from the parents or guardians, as approved by the Institutional Review Board of Cincinnati Children's Hospital Medical Center.

Acknowledgments

This work was supported by NIH grants DK-64008 and DK-83781 (to J.A. Bezerra), DK59427 (to G.J. Gores), and DK78392 (to Y.-H. Wang), and by the Integrative Morphology and the Gene and Protein Expression Cores (DK-789392). We thank Marc E. Rothenberg (Cincinnati Children's Hospital Medical Center, Cincinnati, Ohio, USA) and Andrew N.J. McKenzie (MRC Laboratory of Molecular Biology, Cambridge, United Kingdom) for the *Il13*$^{-/-}$ BALB/c mice, Douglas M. Jefferson (Tufts University School of Medicine, Boston, Massachusetts, USA) for the H69 cell line, and William Balistreri for insightful review of the manuscript.

Received for publication October 15, 2013, and accepted in revised form April 10, 2014.

Address correspondence to: Jorge A. Bezerra, Division of Gastroenterology, Hepatology and Nutrition, Cincinnati Children's Hospital Medical Center, 3333 Burnet Avenue, Cincinnati, Ohio 5229-3030, USA. Phone: 513.636.3008; Fax: 513.636.5581; E-mail: jorge.bezerra@cchmc.org.

1. Bessho K, Bezerra JA. Biliary atresia: will blocking inflammation tame the disease? *Annu Rev Med*. 2011;62:171–185.
2. Razumilava N, Gores GJ. Classification, diagnosis, and management of cholangiocarcinoma. *Clin Gastroenterol Hepatol*. 2013;11(1):13–21.
3. Li J, et al. Th2 signals induce epithelial injury in mice and are compatible with the biliary atresia phenotype. *J Clin Invest*. 2011;121(11):4244–4256.
4. Schmitz J, et al. IL-33, an interleukin-1-like cytokine that signals via the IL-1 receptor-related protein ST2 and induces T helper type 2-associated cytokines. *Immunity*. 2005;23(5):479–490.
5. Moro K, et al. Innate production of T(H)2 cytokines by adipose tissue-associated c-Kit(+)Sca-1(+) lymphoid cells. *Nature*. 2010;463(7280):540–544.
6. Neill DR, et al. Nuocytes represent a new innate effector leukocyte that mediates type-2 immunity. *Nature*. 2010;464(7293):1367–1370.
7. Liew FY, Pitman NI, McInnes IB. Disease-associated functions of IL-33: the new kid in the IL-1 family. *Nat Rev Immunol*. 2010;10(2):103–110.
8. Volarevic V, et al. Protective role of IL-33/ST2 axis in Con A-induced hepatitis. *J Hepatol*. 2012;56(1):26–33.
9. Sakai N, et al. Interleukin-33 is hepatoprotective during liver ischemia/reperfusion in mice. *Hepatology*. 2012;56(4):1468–1478.
10. Liang Y, et al. IL-33 induces nuocytes and modulates liver injury in viral hepatitis. *J Immunol*. 2013;190(11):5666–5675.
11. McHedlidze T, et al. Interleukin-33-dependent innate lymphoid cells mediate hepatic fibrosis. *Immunity*. 2013;39(2):357–371.
12. Monticelli LA, et al. Innate lymphoid cells promote lung-tissue homeostasis after infection with influenza virus. *Nat Immunol*. 2011;12(11):1045–1054.
13. Spits H, et al. Innate lymphoid cells — a proposal for uniform nomenclature. *Nat Rev Immunol*. 2013;13(2):145–149.
14. Halim TY, Krauss RH, Sun AC, Takei F. Lung natural helper cells are a critical source of Th2 cell-type cytokines in protease allergen-induced airway inflammation. *Immunity*. 2012;36(3):451–463.
15. Wong SH, et al. Transcription factor RORα is critical for nuocyte development. *Nat Immunol*. 2012;13(3):229–236.
16. Halim TY, MacLaren A, Romanish MT, Gold MJ, McNagny KM, Takei F. Retinoic-acid-receptor-related orphan nuclear receptor α is required for natural helper cell development and allergic inflammation. *Immunity*. 2012;37(3):463–474.
17. Zhao A, et al. and Shea-Donohue T. Immune regulation of protease-activated receptor-1 expression in murine small intestine during Nippostrongylus brasiliensis infection. *J Immunol*. 2005;175(4):2563–2569.
18. Fan B, et al. Cholangiocarcinomas can originate from hepatocytes in mice. *J Clin Invest*. 2012;122(8):2911–2915.
19. Li H, et al. Deregulation of Hippo kinase signalling in human hepatic malignancies. *Liver Int*. 2012;32(1):38–47.
20. Spence JR, et al. Sox17 regulates organ lineage segregation of ventral foregut progenitor cells. *Dev Cell*. 2009;17(1):62–74.
21. Walker JA, McKenzie AN. Development and function of group 2 innate lymphoid cells. *Curr Opin Immunol*. 2013;25(2):148–155.
22. Monticelli LA, Sonnenberg GF, Artis D. Innate lymphoid cells: critical regulators of allergic inflammation and tissue repair in the lung. *Curr Opin Immunol*. 2012;24(3):284–289.
23. Chang YJ, et al. Innate lymphoid cells mediate influenza-induced airway hyper-reactivity independently of adaptive immunity. *Nat Immunol*. 2011;12(7):631–638.
24. Koyasu S, Moro K, Tanabe M, Takeuchi T. Natural helper cells: a new player in the innate immune response against helminth infection. *Adv Immunol*. 2010;108:21–44.
25. Saenz SA, et al. IL25 elicits a multipotent progenitor cell population that promotes T(H)2 cytokine responses. *Nature*. 2010;464(7293):1362–1366.
26. Han Y, et al. Recent advances in the morphological and functional heterogeneity of the biliary epithelium. *Exp Biol Med*. 2013;238(5):549–565.
27. Werneburg NW, Yoon JH, Higuchi H, Gores GJ. Bile acids activate EGF receptor via a TGF-alpha-dependent mechanism in human cholangiocyte cell lines. *Am J Physiol Gastrointest Liver Physiol*. 2003;285(1):G31–G36.
28. Grubman SA, et al. Regulation of intracellular pH by immortalized human intrahepatic biliary epithelial cell lines. *Am J Physiol*. 1994; 266(6 pt 1):G1060–G1070.
29. Maruyama T, et al. Control of the differentiation of regulatory T cells and T(H)17 cells by the DNA-binding inhibitor Id3. *Nat Immunol*. 2011;12(1):86–95.
30. Verri WA Jr, et al. IL-33 mediates antigen-induced cutaneous and articular hypernociception in mice. *Proc Nat Acad Sci U S A*. 2008;105(7):2723–2728.